Cell, Vol. 112, 845–857, March 21, 2003, Copyright ©2003 by Cell Press

A Myristoyl/Phosphotyrosine Switch Regulates c-Abl

Oliver Hantschel,[1,5] Bhushan Nagar,[3,5] Sebastian Guettler,[1] Jana Kretzschmar,[1] Karel Dorey,[1,6] John Kuriyan,[3,4,*] and Giulio Superti-Furga[1,2,*]

[1]Developmental Biology Programme
European Molecular Biology Laboratory
[2]Cellzome AG
Meyerhofstrasse 1
69117 Heidelberg
Germany
[3]Howard Hughes Medical Institute
Department of Molecular and Cell Biology
Department of Chemistry
University of California, Berkeley
[4]Physical Biosciences Division
Lawrence Berkeley National Lab
Berkeley, California 94720

Summary

The c-Abl tyrosine kinase is inhibited by mechanisms that are poorly understood. Disruption of these mechanisms in the Bcr-Abl oncoprotein leads to several forms of human leukemia. We found that like Src kinases, c-Abl 1b is activated by phosphotyrosine ligands. Ligand-activated c-Abl is particularly sensitive to the anti-cancer drug STI-571/Gleevec/imatinib (STI-571). The SH2 domain-phosphorylated tail interaction in Src kinases is functionally replaced in c-Abl by an intramolecular engagement of the N-terminal myristoyl modification with the kinase domain. Functional studies coupled with structural analysis define a myristoyl/phosphotyrosine switch in c-Abl that regulates docking and accessibility of the SH2 domain. This mechanism offers an explanation for the observed cellular activation of c-Abl by tyrosine-phosphorylated proteins, the intracellular mobility of c-Abl, and it provides new insights into the mechanism of action of STI-571.

Introduction

Cellular regulation and signal transduction often result in the modulation of the activity of protein kinases, the agents of most of the ensuing changes (Brasher and Van Etten, 2000; Schlessinger, 2000; Hubbard and Till, 2000). Thus, different forms of the 518 protein kinases encoded by the human genome (Manning et al., 2002) have adopted a great number of variations of a limited set of fundamental regulatory options, usually involving conformational changes and differential alignment of catalytic residues. In addition to regulation through phosphorylation-dependent conformational changes in the activation loop, located between the two lobes that form the kinase domain, these mechanisms include the alteration of the relative orientation and stiffness of the two lobes relative to one another, the blockage of substrate or ATP access, and changes in subcellular localization and degradation (Cox et al., 1994; Huse and Kuriyan, 2002; Hubbard, 2002).

Among the best understood of the protein kinases in terms of their autoinhibitory mechanism are the Src kinases, a prominent family of nonreceptor tyrosine kinases (Hubbard, 1999; Blume-Jensen and Hunter, 2001). Src kinases are tightly regulated by phosphorylation at a conserved tyrosine in the C-terminal tail of the molecule. C-terminal phosphorylation causes the intramolecular engagement of the enzyme's own SH2 domain with the phosphorylated tail (Sicheri et al., 1997; Xu et al., 1997; Williams et al., 1997). This results in the binding of the SH3 domain to a region linking the SH2 and kinase domains (SH2-kinase linker), a dislocation of the αC-helix in the kinase domain, a closure of the small N-terminal and large C-terminal kinase lobes, and an unproductive conformation of the activation loop. These changes are incompatible with high catalytic activity (Gonfloni et al., 1997, 1999).

Activation of the Src kinases can occur by interfering with this inactive conformation through binding of ligands to the SH3 domain, competing with high-affinity phosphotyrosine ligands for the SH2 domain, and phosphorylating the activation loop tyrosine (Moarefi et al., 1997; Gonfloni et al., 2000; Porter et al., 2000; Liu et al., 1993; Roussel et al., 1991). These features make the Src kinases efficient at integrating various signals, allowing them to act as protein-protein interaction adapters and regulators.

The human *ABL1* and *ABL2* genes encode two tyrosine kinases, c-Abl and Arg, which are closely related to the Src kinases (Van Etten, 1999; Superti-Furga and Courtneidge, 1995; Pendergast, 2002), but display some critical differences: c-Abl and Arg are twice as large as the Src kinases because they contain an additional C-terminal region, encoded by a single exon, which contains nuclear import and export signals as well as several docking sites for cellular proteins, including signaling adapters and actin. c-Abl is expressed in two alternatively spliced forms, 1a and 1b, which differ in the lengths of their first exon regions (Smith and Mayer, 2002). The 1b form is 19 residues longer, contains a myristoylation signal, and seems to be expressed in all cell types (Renshaw et al., 1988).

The cellular activity of c-Abl is normally low (Pendergast, 2002; Smith and Mayer, 2002; Van Etten, 1999). Mutagenesis studies based on the structure of the Src kinases led to the proposal that Abl and Arg are regulated by essentially the same set of intramolecular interactions that govern the Src kinases (Barilá and Superti-Furga, 1998; Pluk et al., 2002). What is achieved by engagement of the tail with the SH2 domain in Src kinases may in c-Abl be replaced by interaction of a

*Correspondence: superti@embl-heidelberg.de (G.S.-F.), kuriyan@uclink.berkeley.edu (J.K.)
[5]These authors contributed equally to this work.
[6]Present address: Cancer Research UK, London Research Institute, 44 Lincoln's Inn Fields, WC2A 3PX London, United Kingdom.

unique N-terminal "cap" with the rest of the molecule (Pluk et al., 2002; Sawyers, 2002; Hubbard, 2002).

Although the architecture of the inactive form was not revealed by these studies, they demonstrated that the minimal region required for c-Abl regulation includes only the first half of the molecule, comprising the cap and the SH3, SH2, and kinase domains. This pointed to a new strategy for the structural analysis of the minimal elements of c-Abl regulation, focused on the first ~530 residues of the protein. In the process of purifying this autoinhibited smaller form of c-Abl, we noticed that the protein was fully myristoylated, as expected, but extremely soluble. The ensuing structure-function analysis resulted in the determination of three crystal structures of Abl (Nagar et al., 2003 [this issue of *Cell*]) and in the definition of a myristoyl and SH2-domain dependent switch that allows c-Abl to be regulated, like Src-kinases, by phosphotyrosine-containing ligands.

Results

Myristoylation Is Critical for c-Abl Regulation

c-Abl has been shown to be myristoylated, as predicted by its primary structure, on the glycine residue at position 2 (Jackson and Baltimore, 1989; Resh 1999). We purified recombinant variants of the minimal regulated form of c-Abl 1b from insect cells for crystallization trials and tested their activity. Surprisingly, Abl forms in which the glycine at position 2 had been mutated to alanine (G2A mutation) displayed dramatically higher activity than wild-type c-Abl and was not myristoylated, as confirmed by mass spectrometry (data not shown).

Also, expression of full-length c-Abl bearing the G2A mutation in HEK 293 cells resulted in high cellular phosphotyrosine levels. The Abl G2A protein was strongly phosphorylated, in contrast to c-Abl wild-type (Figures 1A and 1B), presumably by autophosphorylation (Brasher and Van Etten, 2000; Dorey et al., 2001). Abl G2A also displayed high in vitro tyrosine kinase activity with either GST-Crk or an optimal peptide as substrate (Zhou et al., 1995; data not shown and see below). The activity of Abl G2A was comparable to that of Abl PP, a deregulated form in which two prolines in the SH2-kinase linker are mutated (P242E/P249E) (Barilá and Superti-Furga, 1998). Combination of the G2A and the PP mutation (Abl G2A/PP) resulted in a form of the kinase that was even more active than forms of c-Abl containing either of the individual mutations (Figure 1B). These results suggested an unexpected involvement of the myristoyl modification in c-Abl regulation.

Abl PP and Abl G2A displayed very similar affinities for the substrate (K_M of 16 μM and 13 μM, respectively) and similar maximum velocities (v_{max} 7.4 pmol/min and 6.5 pmol/min, respectively, Figure 1C). Thus, mutation of the myristoyl acceptor site activated c-Abl as much as the mutation in the SH2-kinase linker (Abl PP), which was previously the most activating of the c-Abl mutations. c-Abl, in contrast, showed a higher K_M (95 μM) and lower v_{max} (3.8 pmol/min). Interestingly, the G2A/PP mutant protein had a lower K_M (9 μM) than Abl PP or Abl G2A and a higher v_{max} (8.7 pmol/min), showing the synergism between SH3 docking and the effect of the myristoyl group.

A Functional Requirement for the Myristoyl Binding Pocket

Purification of the minimal c-Abl 1b construct that is autoregulated (residues 1–531) from insect cells unexpectedly produced extremely soluble myristoylated protein. This suggested that the myristoyl modification might be sequestered within the rest of the protein. We performed isothermal titration calorimetry (ITC), using the isolated Abl kinase domain (Nagar et al., 2002; Schindler et al., 2000) and a myristoylated peptide corresponding to the residues of the very N terminus of c-Abl 1b. We added STI-571 to the kinase domain since this is thought to improve its stability. This peptide bound to the kinase domain of c-Abl with an affinity of 2 μM, while a peptide with the same sequence but lacking the myristoyl group did not bind (Figure 2A and data not shown). This result strongly indicated that the kinase domain of c-Abl has a binding site for the myristoyl group and led us to determine the crystal structure of the Abl kinase domain in complex with a myristoylated peptide. The crystal structure as well as two structures of larger c-Abl constructs showed the myristoyl group bound in a deep hydrophobic pocket at the base of the kinase domain (Figures 2B and 2C; Nagar et al., 2003). Four α helices form a deep cleft covered by the $\alpha I'$-helix, which is positioned as a lid on top of the pocket (Figure 2C). In order to test whether exclusion of the myristoyl group from this pocket in the kinase domain led to a similar level of activation as does the prevention of myristoylation, we mutated residues located within this pocket, introducing either bulkier side chains or polar residues into its hydrophobic environment (Figure 2C).

Forms of full-length c-Abl 1b bearing the A356N and V525D mutations were highly active, whereas the I521D, A452L, and F516N mutants were only slightly more active than c-Abl (Figure 2D). While none of the single point mutations resulted in an activity comparable to that of the G2A form, deletion of the entire $\alpha I'$-helix (ΔE517-K527) led to an activation comparable to that seen for the G2A form lacking the myristoyl group.

Deregulation of Abl G2A Is Not Due to Changes in Localization

N-myristoylation is often important in targeting proteins to membranes (Resh, 1999). In order to test whether the high activity observed for the G2A mutant is due to altered subcellular localization we performed confocal immunofluorescence microscopy with transfected VERO monkey cells, which are particularly well-suited for microscopy due to their large size and flat shape. Under the settings used, endogenous c-Abl could hardly be detected (data not shown). All four forms of transfected c-Abl (c-Abl, Abl PP, Abl G2A, and Abl G2A/PP) were abundant in the cytoplasm, and only a minor fraction was found in the nucleus (Figure 3A, left). Costaining of the cells for F-actin suggested that the prominent surface signal of Abl observed in all cells was due to colocalization of Abl with the cortical actin cytoskeleton (Figure 3A, right two panels; Van Etten et al., 1994). Abl G2A was localized similarly to c-Abl, as were Abl PP and Abl G2A/PP. Similar results were obtained when using HeLa and HEK 293 cells (data not shown).

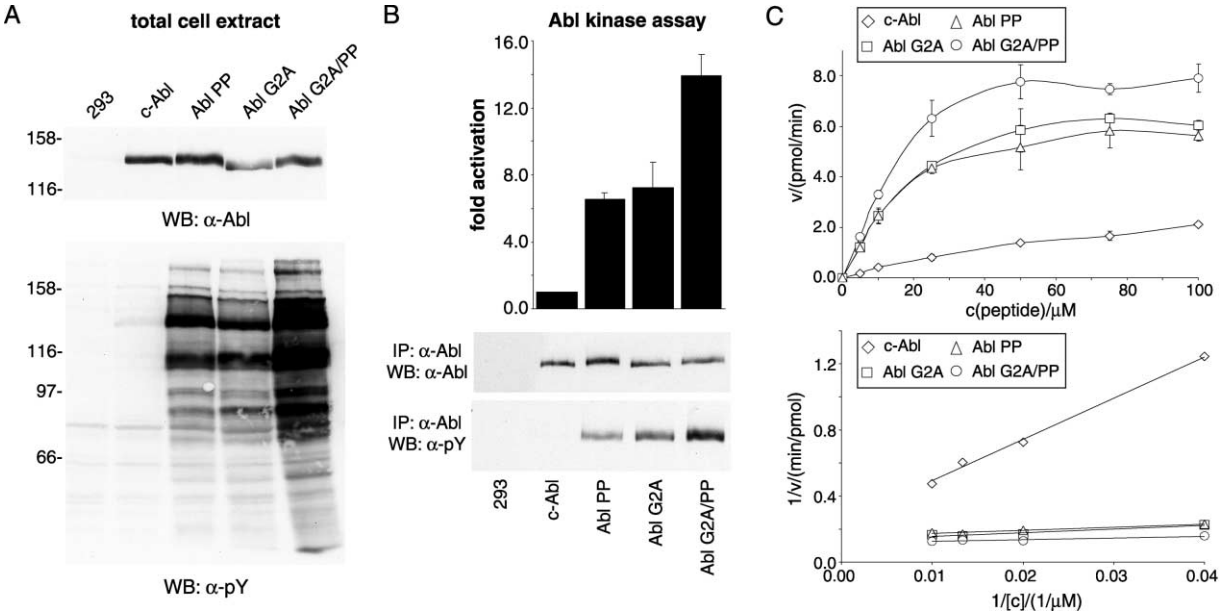

Figure 1. Myristoylation Is Critical for c-Abl Regulation

(A) HEK 293 cells were transiently transfected with the indicated SV40-driven Abl expression constructs. Cells were lysed 40 hr after transfection and total protein extracts analyzed by anti-Abl and anti-phosphotyrosine immunoblotting.

(B) Abl immunoprecipitates were probed with anti-Abl and anti-phosphotyrosine antibodies (lower panels) and assayed for catalytic activity by in vitro kinase assays using an optimal substrate peptide. The histograph shows the catalytic activity (mean with S.D. of three experiments done in duplicate) of the Abl constructs relative to c-Abl and corrected for endogenous c-Abl levels.

(C) Immunoprecipitated Abl proteins were assayed for catalytic activity in the presence of 100 μM ATP and the indicated concentrations of an optimal substrate peptide. Specific activity was calculated and plotted over the substrate concentration (Michaelis-Menten graph, top). The graph shows the mean with S.D. of two experiments done in duplicate. The double-reciprocal plot (Lineweaver-Burk plot) was used to calculate K_m and v_{max}.

In order to get more quantitative insight into the subcellular localization of c-Abl, HEK 293 cells expressing the same forms of Abl as used for microscopy were fractionated into extracts enriched in nuclear, cytosolic, or membrane proteins by differential velocity centrifugation. Equivalent amounts of total protein were used for detection of Abl in immunoblots (Figure 3B, top). Parallel immunodetection of nuclear (RCC1), cytosolic (β-actin), and membrane (presenilin-1) proteins confirmed the purity of the fractions (Figure 3B, bottom). In all cases, the ratio of the total amount of Abl protein to the amount of Abl found in a particular fraction was the same for the wild-type and mutant proteins. These observations support the view that the observed dramatic increase in c-Abl activity upon removal of the myristoyl group was not due to a different localization of the bulk of the protein.

Proper Regulation of c-Abl Forms Containing a Shortened N-Terminal Cap

The importance of myristoylation in the regulation of c-Abl raised the question as to whether the previously analyzed cap region mainly serves as an unstructured and nonspecific bridge between the myristoyl group and the base of the kinase domain (Pluk et al., 2002). To identify the minimal requirements for cap function, we introduced a series of point mutations and deletions into the region (Figure 4A). Previous results have shown that two mutant forms of c-Abl 1b, cap1 (amino acids 7–10 to alanine) and cap6 (amino acids 70–73 to alanine) are deregulated (Pluk et al., 2002). We mutated each of the residues in cap1 and cap6 individually. Within the cap1 region, only the K7A mutant was activating (data not shown). Since positively charged residues at position 7 are necessary for N-myristoylation, the K7A mutation may be impairing myristoylation of c-Abl. On the other hand, three single point mutations in the cap6 region (E71A, N72A, and L73A) resulted in a moderate increase in activity and one, K70A, was almost as active as Abl PP (Figure 4B).

An alignment of the cap regions of c-Abl 1b and c-Abl 1a (Figure 4A) prompted us to speculate that stretches of residues between the conserved parts of the two alternative spliceforms (regions L1 and L2 in c-Abl 1b) could loop out from a minimal link between the SH3 domain and the myristoyl binding site and, therefore, be dispensable for autoinhibition. Indeed, Abl forms with the L1, L2, L3, L4, or L5 regions deleted did not show significantly higher catalytic activity or levels of autophosphorylation compared to c-Abl (data not shown). While even larger deletions of up to 45 amino acids (ΔL1-L5) did not lead to any increase in c-Abl activity, a deletion of 54 residues (ΔL1-L6) activated the kinase (Figure 4D). The form of c-Abl with the largest deletion in the cap and still properly regulated (ΔL1-L5) was still dependent on myristoylation, as shown by the strong increase in activity that results when the G2A mutation is combined with this deletion (G2A/ΔL1-L5, Figure 4D). Interestingly, an increase in kinase activity was also seen

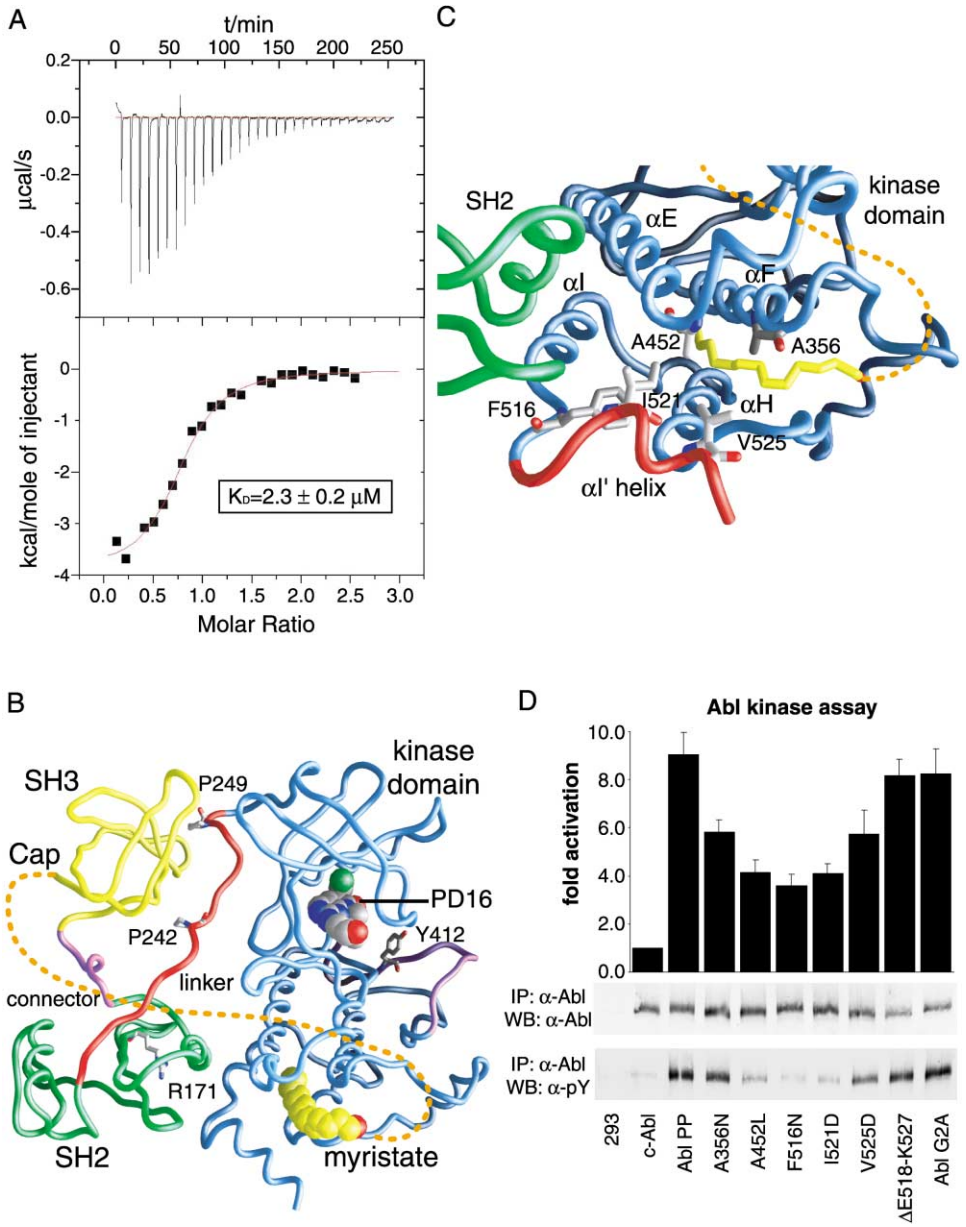

Figure 2. Myristoyl Binds a Hydrophobic Pocket in the Kinase Domain

(A) Isothermal titration calorimetry measuring binding of the purified Abl kinase domain to a myristoylated c-Abl 1b peptide (Myr-GQQPGKVLGDQRRPSL). Top, raw data of the titration; bottom, integrated heats of injections, corrected for the heat of dilution.

(B) Backbone worm representation of the crytstal structure of myristoylated c-Abl 1b (residues 2–531) in complex with the inhibitor PD16. The N-terminal myristoyl moiety is sequestered in a hydrophobic pocket in the large lobe of the kinase domain. Dotted lines indicate the N-terminal cap (residues 2–79), which was disordered in the crystal. Some critical residues are labeled and shown as rod models. Tyr-412 specifies the activation loop phosphorylation site; Pro-242 and Pro-249 are mutated in Abl PP, and Arg-171 indicates the phosphotyrosine binding site in the SH2 domain. The inhibitor PD16 and the N-terminal myristoyl are shown as CPK models.

(C) Closeup view of the myristoyl binding pocket in the large lobe of the kinase domain. The myristoyl is indicated in yellow, and key hydrophobic residues that we have mutated are labeled and shown as rod models. The αI′-helix (residues E518–K527) is highlighted in red.

(D) The indicated Abl myristoylation pocket mutants were transiently expressed in HEK 293 cells. Anti-Abl immunoprecipitates were analyzed by anti-Abl and anti-phosphotyrosine immunoblotting (bottom) and assayed for catalytic activity by in vitro kinase assays (top). The histograph shows the fold activation of the indicated constructs compared to c-Abl (mean with S.D. of three experiments done in duplicate) and corrected for endogenous c-Abl.

upon combining the G2A mutation with the K70A mutation in the intact cap, suggesting that the cap does not only function in presenting the myristoyl group (Figure 4D).

In summary, only some 30 of the 80 residues linking the myristoyl group to the SH3 domain appear to be required for regulation. Within this minimal cap, an essential element consists of the myristoyl group with its

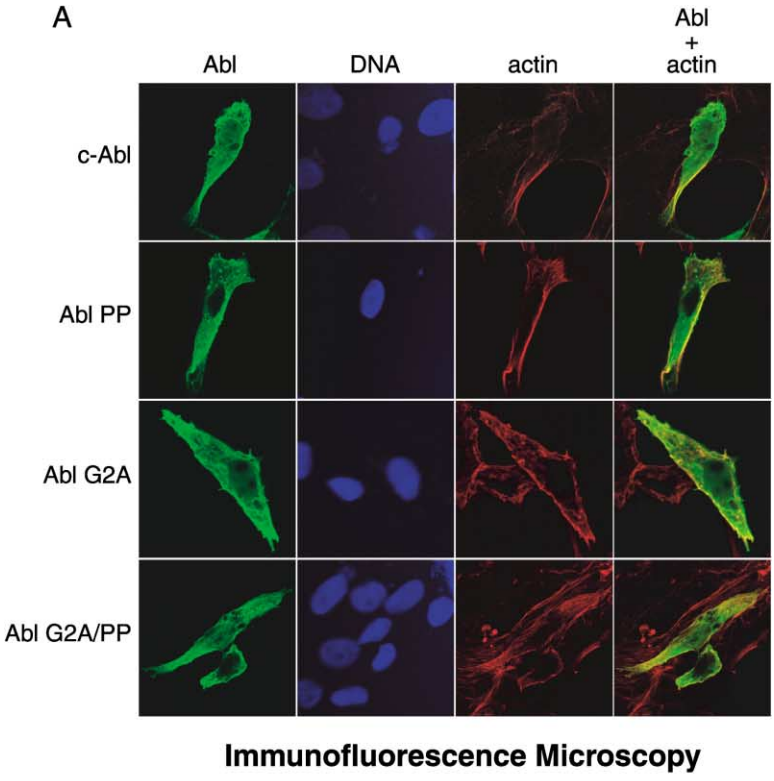

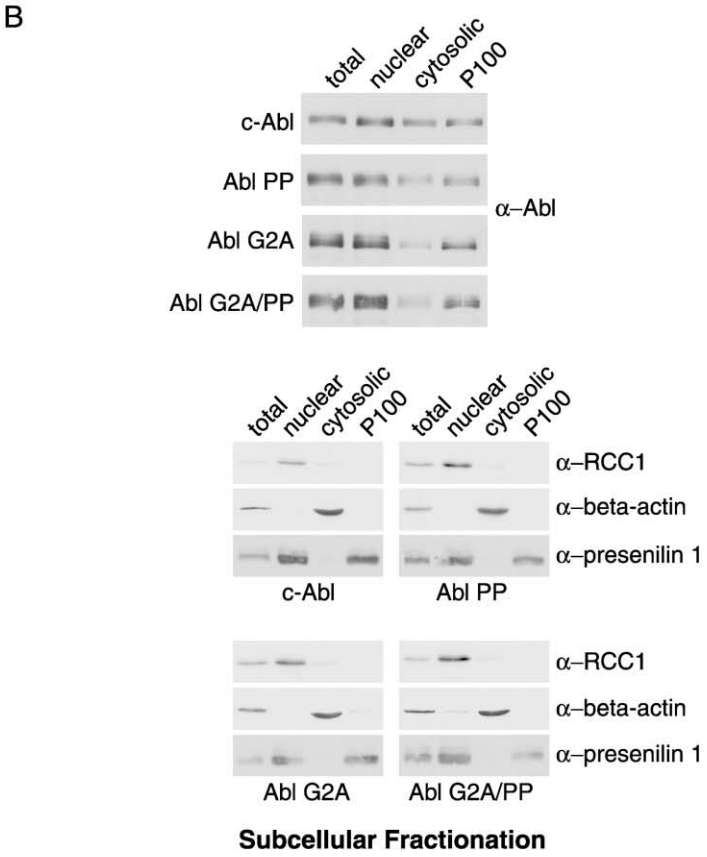

Figure 3. Subcellular Localization of Abl

(A) VERO cells were transiently transfected with the indicated Abl expression constructs, fixed 40 hr later, and immunostained with an anti-Abl antibody (first panel). DNA was stained with DAPI (second panel), and colocalization of Abl with actin was revealed using phalloidin-rhodamine (third panel, actin; fourth panel, merge Abl and actin). Images show 1 μm confocal sections in the midnuclear planes.

(B) HEK 293 cells transiently transfected with the indicated Abl constructs were fractionated by differential velocity centrifugation. Equal protein amounts were analyzed by immunoblotting using an anti-Abl antibody (top) and antibodies against marker proteins for the different subcellular compartments (bottom; nuclear marker, RCC1; cytosolic marker, β-actin; membrane marker, presenilin-1). P100 indicates the crude membrane fraction.

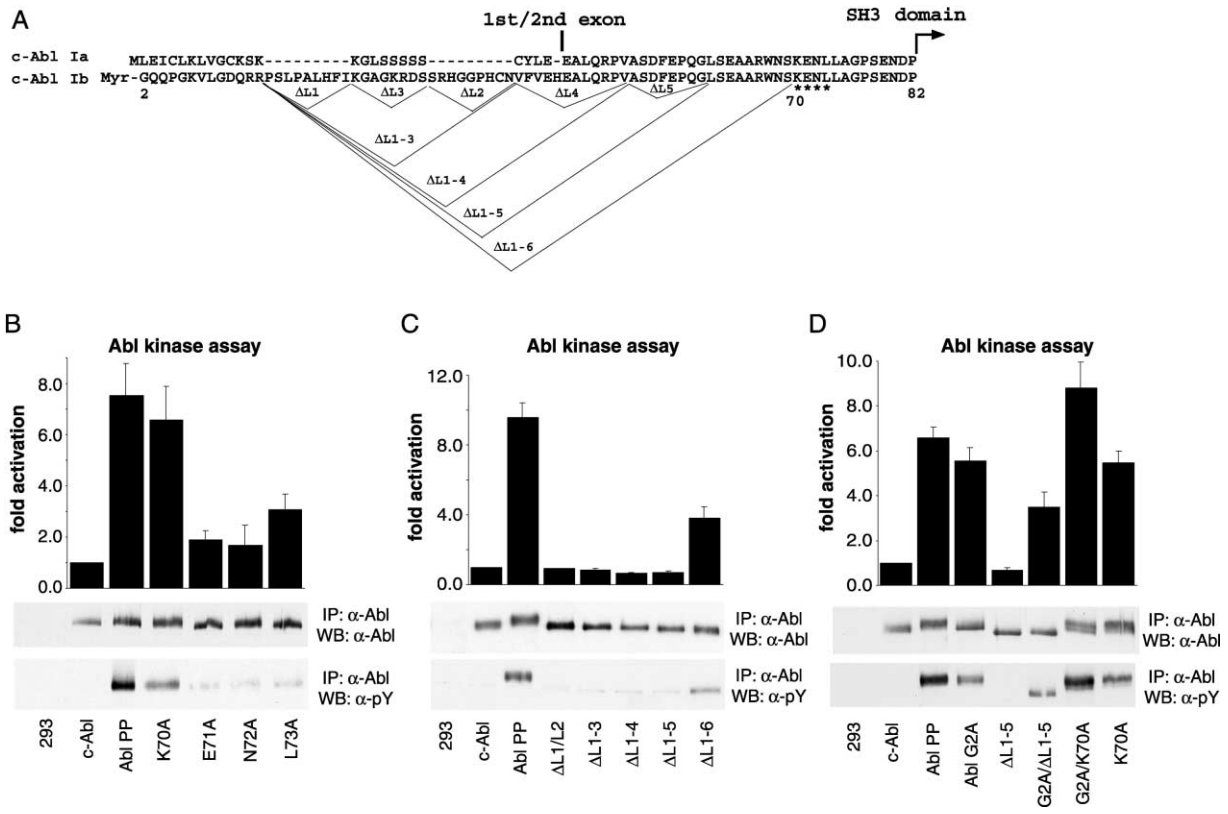

Figure 4. Mutational Analysis of the N-Terminal Cap

(A) Alignment of the c-Abl type 1a and 1b N-terminal cap regions (exons 1 and 2). Residues K70–L73 are labeled with asterisks. Deletion mutants are indicated.

(B–D) The indicated Abl cap mutants were transiently expressed in HEK 293 cells. Anti-Abl immunoprecipitates were analyzed by anti-Abl and anti-phosphotyrosine immunoblotting (bottom) and assayed for catalytic activity by in vitro kinase assays using an optimal substrate peptide (top). The histograph shows the fold activation of the different constructs compared to c-Abl (mean with SD of two experiments done in duplicate) and corrected for endogenous c-Abl.

corresponding recognition motif for the N-Myristoyltransferase (including Lys-7), and a second critical region comprises Lys-70, as well as Leu-73, proximal to the first β strand of the SH3 domain (Musacchio et al., 1994).

Activation by Phosphotyrosine Ligands

During the course of our investigations, we discovered that phosphopeptides are capable of activating c-Abl. This finding could not be reconciled with currently known mechanisms of c-Abl activation. To investigate this phenomenon systematically, we treated c-Abl with phosphopeptides derived from two c-Abl substrates known to bind the Abl SH2 domain (Barilá et al., 2000; Zhu et al., 1994). As controls, we used peptides of the same sequence in which the phosphotyrosine was replaced by a phenylalanine as well as an Abl form bearing a point mutation in the SH2 phosphotyrosine binding site (Abl R171L, FLVR motif), which renders the SH2 domain incompetent for binding phosphotyrosine (Mayer et al., 1992).

We observed a concentration-dependent increase in c-Abl activity when the wild-type protein is treated with either of the two phosphopeptides (Figure 5A). Treatment of wild-type c-Abl with the mutated control peptides had no effect, suggesting phosphotyrosine-dependence of the activation. Moreover, Abl R171L did not show any increase in kinase activity when treated with the phosphopeptides or the control peptides, demonstrating that the activation requires a functional SH2-domain.

This finding is explained by the crystal structures of regulated c-Abl, in which the SH2 domain packs against the kinase domain in a way that partly occludes the ligand binding site. Specifically, although the phosphotyrosine binding site of the SH2 domain is largely accessible, the kinase domain impairs binding by masking the binding sites for the residues immediately upstream of the phosphotyrosine (Nagar et al., 2003).

To evaluate the accessibility of the SH2 domain in regulated c-Abl compared to active forms (Abl PP and Abl G2A), we determined the affinities of phosphopeptide ligands for the SH2 domain by isothermal titration calorimetry (ITC). c-Abl wild-type displayed a higher K_D than the active forms Abl PP and Abl G2A. We also detected lower binding stoichiometry for the wild-type protein compared to its active counterparts (Table 1 and data not shown). These observations indicated that the

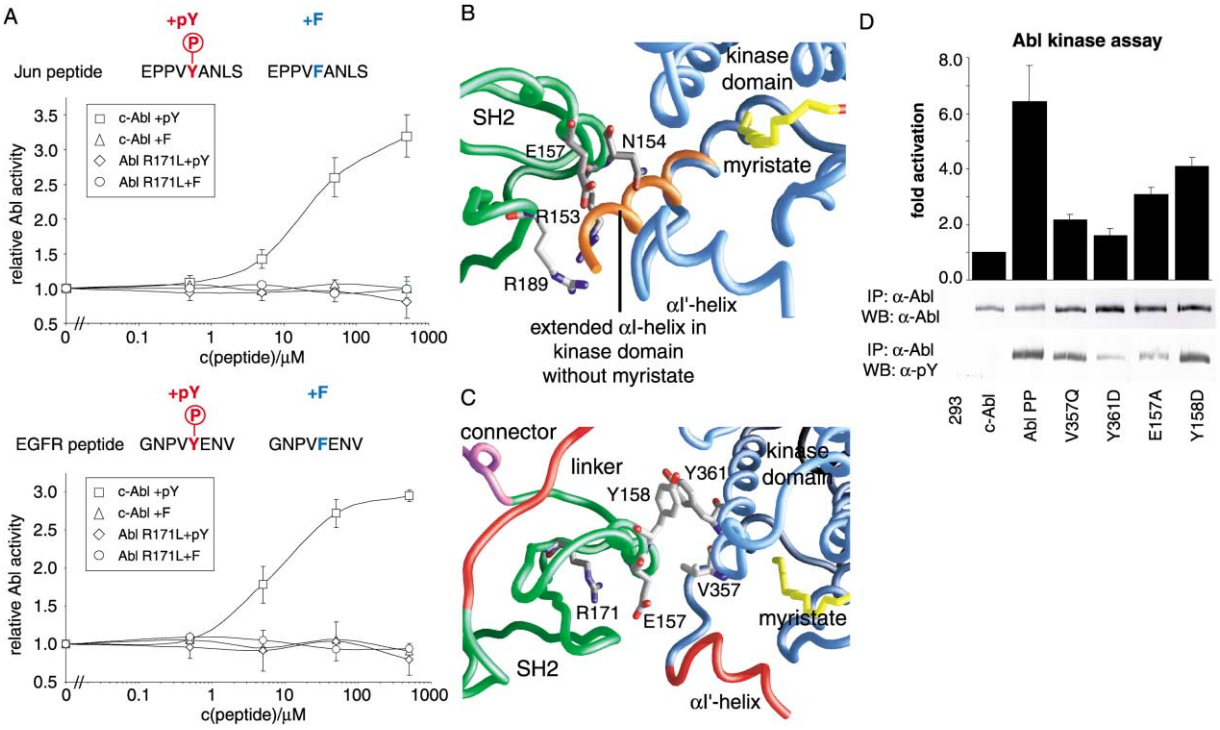

Figure 5. Positioning of the SH2 Domain and SH2 Domain-Dependent Regulation of c-Abl

(A) Immunoprecipitated c-Abl or Abl R171L was preincubated with the indicated concentrations of either phosphopeptide (+pY) or a control peptide (+F). Abl catalytic activity was determined using an optimal substrate peptide. The results were normalized for the reaction in the absence of phosphopeptide or control peptide, and relative Abl activity was calculated. The graph shows the mean with S.D. of three independent experiments done in duplicate or triplicate for the Jun peptide (top) and the mean with S.D. of two independent experiments done in duplicate for the EGFR peptide (bottom).

(B) Backbone worm representation of regulated c-Abl. The structure of the Abl kinase domain with an unoccupied myristoyl binding pocket (PDB entry 1M52; Nagar et al., 2002) is superimposed onto the regulated c-Abl structure. The αI-helix of the myristoyl-free Abl kinase domain, shown in orange, clashes with the SH2 domain. Key residues in the SH2 domain are shown as rod models.

(C) Backbone worm representation of the SH2-kinase domain interface in c-Abl. Key residues that we have mutated are labeled and shown as rod models.

(D) The SH2-kinase domain interface mutants were transiently expressed in HEK 293 cells. Anti-Abl immunoprecipitates were analyzed by anti-Abl and anti-phosphotyrosine immunoblotting (bottom) and assayed for catalytic activity by in vitro kinase assays using an optimal substrate peptide (top). The histograph shows the fold activation of the different constructs compared to c-Abl (mean with S.D. of two experiments done in duplicate) and corrected for endogenous c-Abl.

phosphotyrosine binding sites of active Abl forms are more accessible than the ones of the wild-type protein.

The SH2-Kinase Domain Interface Is Critical for Autoinhibition

The crystal structures of regulated c-Abl show that the SH2 domain packs tightly against the large lobe of the kinase domain. The αI-helix at the C terminus of the kinase domain without bound myristoyl group (Nagar et al., 2002, Schindler et al., 2000) projects into the space occupied by the SH2 domain in the assembled structure, effectively preventing SH2 domain docking (Figure 5B). The comparison suggests a myristoyl switch mechanism in which binding of the myristoyl group causes the αI-helix to bend and position the αI′-helix as a lid onto the myristoyl binding pocket, thereby rendering the docking site accessible for the SH2 domain. We tested this hypothesis by mutating residues at the SH2-kinase domain interface (Figure 5C). Several mutations showed only minor effects on c-Abl activity (see Supplemental Table S1 online at http://www.cell.com/cgi/content/full/112/6/845/DC1). However, Abl proteins mutated in Glu-157, Tyr-158, Val-357, or Tyr-361 showed an intermediate to strong increase in phosphorylation of cellular proteins on tyrosine (data not shown), autophosphorylation, and kinase activity when mutated (Figure 5D).

These observations demonstrated that the interface between the SH2 and kinase domains is involved in regulating c-Abl and that Tyr-158 in particular may be a key determinant for proper positioning of the SH2 domain.

A Conserved Snap-Lock Mechanism Involving the SH3/2 Connector

Molecular dynamics simulations indicated that the SH3 and SH2 domains in Src family kinases are tightly coupled via a rigid connector and that the connector functions as an inducible snap-lock in Src kinases (Young et al. 2001). In support of this model, replacement of connector residues with glycines leads to a strong activation of c-Src (Young et al., 2001).

Superimposition of the crystal structures of regulated

Table 1. Isothermal Titration Calorimetry (ITC) of Different Abl Mutants with a Phosphopeptide

c-Abl$^{1-531}$ Construct	K_D/μM
Abl D382N	19.1
Abl D382N/PP	7.2
Abl D382N/G2A	7.7

Recombinant proteins were expressed in Sf9 cells and purified in the presence of PD16 (Nagar et al., 2003). Isothermal titration calorimetry (ITC) was performed using a VP-ITC machine (MicroCal). Abl:PD16 complexes and peptide sample (GNPVpYENV; Zhu et al., 1994) were transferred to a buffer containing 20 mM Tris/HCl (pH 8.0), 150 mM NaCl, and 5 mM DTT. Titrations were performed at 25°C by injecting 25–30 consecutive aliquots of 10 μl of peptide solution (1 mM) into the ITC cell containing Abl:PD16 complex (100 μM). The thermodynamic parameters of the reaction were determined by fitting the corrected data to a bimolecular interaction model.

c-Abl and c-Src showed a remarkable overlap of the SH3-SH2 domain clamps, including their SH3/2 connectors (Figure 6A). Moreover, Ser-140 in the connector of c-Abl has been identified as a critical residue in a random screen for c-Abl activating mutants (Brasher et al., 2001). We tested the effect of a triple glycine mutation (S140G/L141G/E142G) aimed at disrupting the structural rigidity of the connector (Figure 6B). The triple glycine mutant was indeed autophosphorylated, showed high tyrosine kinase activity in vitro and in vivo, and was stronger in activity compared to the S140I mutant used as a control (Figure 6C; Brasher et al., 2001).

These results suggested that the role of the SH3/2 connector in the autoregulatory mechanism is conserved between c-Src and c-Abl. It remains to be determined how uncoupling of the two domains is regulated in wild-type c-Abl, because the molecular uncoupling switch equivalent to the release of the tail phosphotyrosine in c-Src is not evident.

Ligand-Activated c-Abl Has Heightened Sensitivity to STI-571

STI-571 has been demonstrated to inhibit Bcr-Abl and to block c-Abl-dependent actin microspike formation in cells spreading on fibronectin (Druker et al., 1996; Woodring et al., 2002). Crystal structures of Abl bound to this inhibitor have been determined (Nagar et al., 2002, 2003). Whether STI-571 can inhibit c-Abl activity is not known because no experimental protocol to preserve c-Abl regulation in vitro was available until recently (Plattner et al., 1999; Pluk et al., 2002). STI-571 only binds efficiently to the Abl kinase domain when the activation loop tyrosine (Tyr-412) is not phosphorylated (Schindler et al., 2000; Nagar et al., 2002). This conformation is associated with low catalytic activity (Dorey et al., 2001).

We determined the catalytic activity of immunoprecipitated c-Abl wild-type and Abl PP in the presence of various concentrations of STI-571. c-Abl wild-type showed an inhibition curve with an IC_{50} of 400 nM for STI-571. To obtain a form of c-Abl that is released from the inhibitory restraints of the SH3 and SH2 domains but is not already phosphorylated on Tyr-412 like Abl PP, we activated c-Abl allosterically with a phosphopeptide in the absence of ATP. This activated form of c-Abl showed a significantly lower IC_{50} for STI-571 (150 nM) than c-Abl. On the other hand, Abl PP, which is strongly phophorylated on Tyr-412 (Dorey et al., 2001), displayed a higher IC_{50} (800 nM) than c-Abl wild-type (Figure 6D).

Taken together, these data indicated that the conformational state of c-Abl had an impact on the ability of STI-571 to inhibit catalytic activity, as previously suggested (Roumiantsev et al., 2002). The inhibitory SH3/2 clamp appears to counteract binding of STI-571 to the ATP binding site, presumably by restraining movements of the kinase domain lobes relative to each other in the regulated conformation, making it more difficult for the relatively large STI-571 to enter the kinase domain.

Discussion

Important common themes have emerged from the analysis of the regulatory mechanisms of protein kinases, suggesting that kinases that are closely related might share common mechanisms of action (Huse and Kuriyan, 2002; Schlessinger, 2000; Hubbard, 2002; Hubbard and Till, 2000; Taylor and Radzio-Andzelm, 1997; Blume-Jensen and Hunter, 2001). Recent work, as well as the evidence provided by this and the accompanying paper (Nagar et al., 2003) on the structure of regulated c-Abl, shows that the Src and Abl kinases are very similar in their internal control mechanisms (Barilá and Superti-Furga, 1998; Plattner et al., 1999; Brasher et al., 2001; Pluk et al., 2002; Huse and Kuriyan, 2002). Like the Src kinases, c-Abl and its paralogue Arg (S.G., O.H. and G.S.F., unpublished data), are negatively regulated by an intramolecular SH3 domain-mediated interaction "sandwich" involving the linker and the kinase domain and can be activated by phosphorylation of their activation loop (Plattner et al., 1999; Brasher and Van Etten, 2000; Dorey et al., 2001; Furstoss et al., 2002). Most surprisingly, c-Abl is also activated by phosphotyrosine ligands. The implication is that the Src kinases and Abl/Arg are essentially built to execute a core function of transducing protein-protein interaction signals into a phosphorylation signal that generates further protein-protein interactions. Conversely, they engage in protein-protein interactions in response to phosphorylation events that alter the conformation of their kinase domain (Gonfloni et al., 2000; Porter et al., 2000).

Burial of the myristoyl group within the kinase domain may explain why c-Abl is able to shuttle between the nucleus and the cytoplasm, depending on environmental cues, in a manner that had been difficult to reconcile with constitutive membrane association (Taagepera et al., 1998; Van Etten, 1999). In general, myristoylation is not necessarily coincident with membrane association, as there are several myristoylated proteins that are soluble (Resh, 1999; Taniguchi, 1999) and the myristoyl group is insufficient to stably anchor proteins to membranes on its own (Resh, 1994). A different matter altogether is the myristoylation-dependent transforming activity of deregulated forms of c-Abl, like v-Abl. In these cases, activation of membrane bound GTPases, resulting in activation of MAP kinase pathways, appears to be a prerequisite (Daley et al., 1992; McWhirter et al., 1993; Raitano et al., 1997; Feller et al., 1994; Van Etten, 1999).

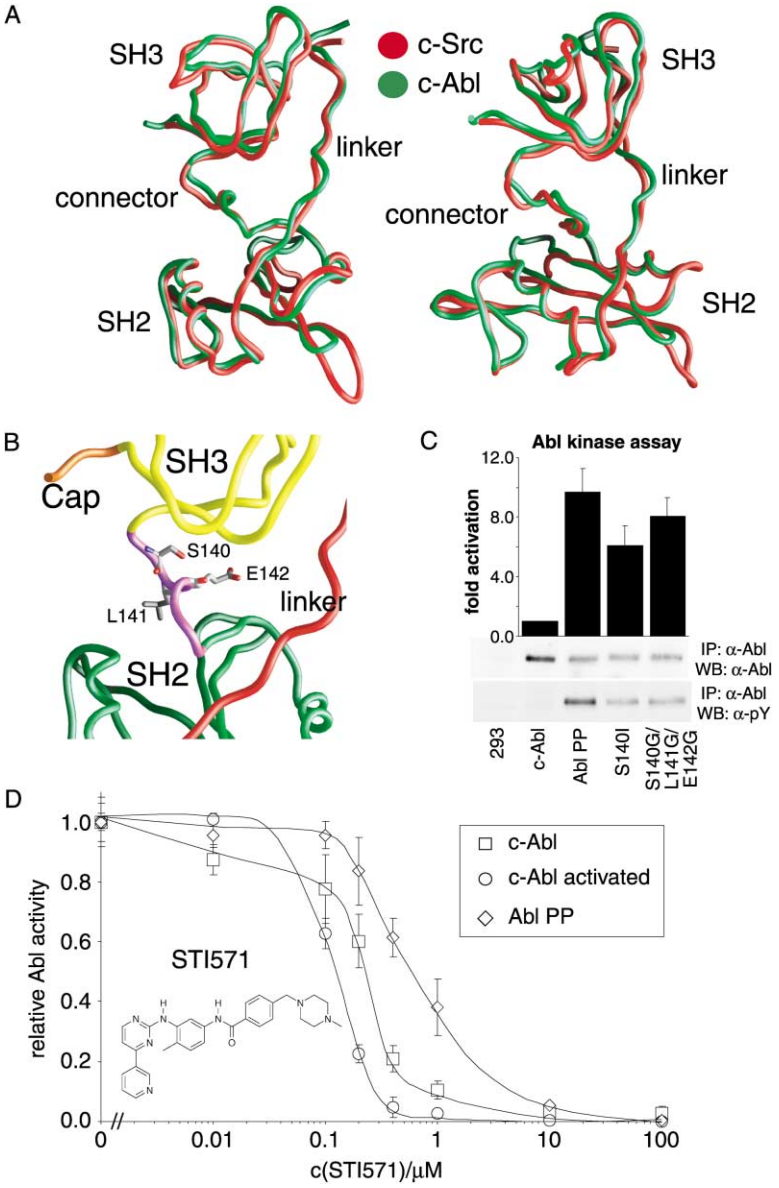

Figure 6. Role of the SH3-SH2 Connector and Inhibition by STI-571

(A) Superimposition of the SH3-SH2 regions of regulated c-Src (red backbone worm; PDB entry 2SRC) and c-Abl (green backbone worm) in two different orientations. The right panel shows a view that is rotated 45° counterclockwise around the vertical axis.

(B) Closeup view of the SH3-SH2 connector in regulated c-Abl. Residues that we have mutated are labeled and shown as rod models.

(C) The connector mutants were transiently expressed in HEK 293 cells. Anti-Abl immunoprecipitates were analyzed by anti-Abl and anti-phosphotyrosine immunoblotting (bottom) and assayed for catalytic activity by in vitro kinase assays using an optimal substrate peptide (top). The histograph shows the fold activation of the different constructs compared to c-Abl (mean with S.D. of two experiments done in duplicate) and corrected for endogenous c-Abl.

(D) c-Abl or Abl PP protein was immunoprecipitated (for the c-Abl and Abl PP control reactions) or immunoprecipitated and activated with phosphopeptide (c-Abl activated). STI-571 was added at the indicated concentrations. Catalytic activity was determined and normalized for the reaction in the absence of STI-571. The graph shows the mean with S.D. of three independent experiments done in duplicate. The chemical structure of the inhibitor is indicated.

A critical question left open concerns the active role of myristoylation in normal c-Abl function. Does the myristoyl group ever leave the pocket? Are there dedicated proteins sequestering it? The alternatively spliced form c-Abl 1a is 19 residues shorter and not myristoylated. Both forms can independently rescue the defects caused by c-Abl gene knockout (Hardin et al., 1996), suggesting that myristoylation does not have an irreplaceable role in the cellular function of c-Abl. c-Abl bearing the type 1a exon is equally well regulated in vitro and in vivo when expressed in HEK 293 cells (O.H. and G.S.F., unpublished data). The elements of Abl 1a that replace the action of the myristoyl group in Abl 1a remain to be determined.

The most dramatic effect of the interaction of the myristoyl group and the kinase domain appears to be the gating effect on SH2 docking. Given the network of SH2-kinase domain interactions and the snap-lock mechanism of the SH3/SH2 clamp, c-Abl is activated, like the Src kinases, by phosphotyrosine ligands. This surprising finding offers an explanation for two phenomena that have remained unexplained: activation of c-Abl by high concentration of substrates and dependence on the SH2 domain for efficient phosphorylation by c-Abl (Smith and Mayer, 2002). c-Abl substrates may initially be phosphorylated through the basal kinase activity of c-Abl or other kinases and initiate a positive feedback loop involving SH2 domain-dependent activation of c-Abl and resulting in facilitated substrate recruitment. This may not only form the basis for our previous insights into the nuclear tyrosine phosphorylation circuit involving c-Abl, its substrate c-Jun, and JNK (Barilá et al., 2000), but may also account for findings involving activation by Abl interactor 1, Nck, paxillin, Cbl, γ-PAK, Cables, and possibly also p73, c-Crk, Ena (enabled), disabled, and many other proteins (reviewed in Pendergast, 2002). In addition to the proposed role for the SH2 domain in increasing the processivity of the enzyme (Smith and

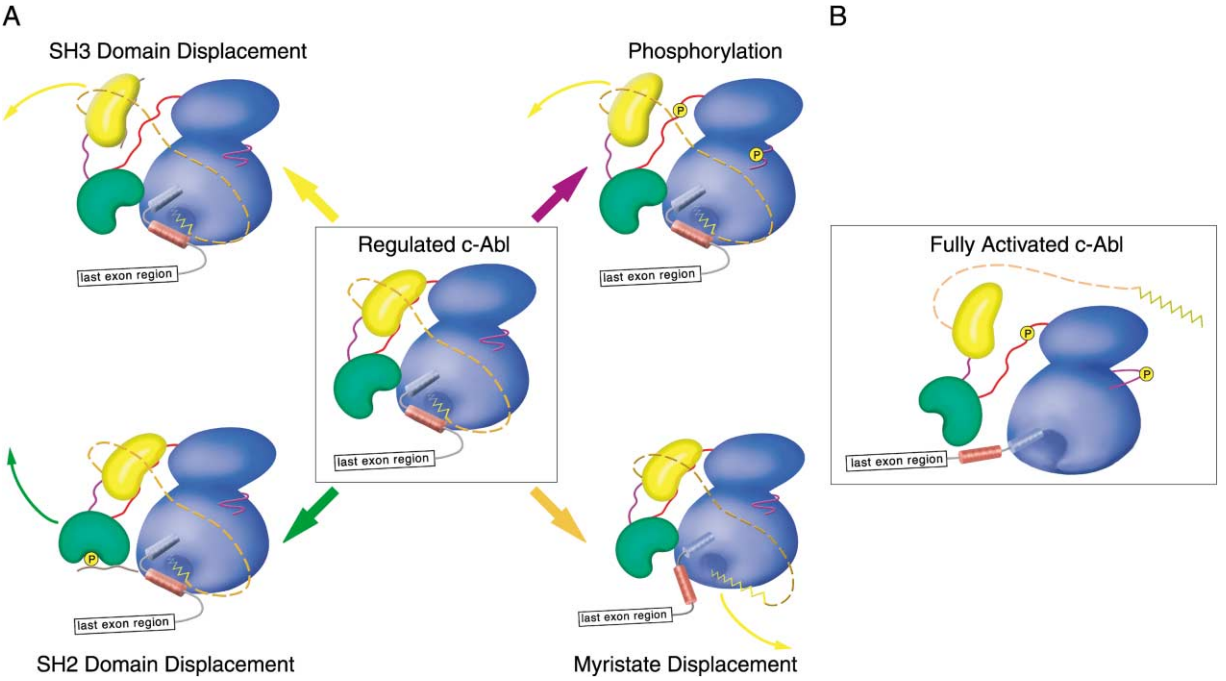

Figure 7. Schematic Representation of c-Abl Activation Modes

(A) Schematic representation of regulated c-Abl 1b (center). The domains and linkers are colored as in all other figures. Surrounding the central figure, four potential activation mechanisms for c-Abl 1b and their concomitant potential domain rearrangements are shown: SH3 domain-dependent activation (upper left), SH2 domain-dependent activation (lower left), activation by phosphorylation on Tyr-412 (activation loop) or Tyr-245 (SH2-kinase linker) (upper right), and activation by myristoyl displacement (lower right).

(B) Schematic representation of fully active c-Abl 1b.

Mayer, 2002), phosphotyrosine ligands can shift c-Abl into an active conformation, preventing it from reassuming the regulated, inhibited conformation. In agreement with this hypothesis, it has been reported that c-Abl binds to receptor tyrosine kinases, such as EphB2 (Yu et al., 2001) and Trk (Yano et al., 2000), as well as to the B cell receptor ancillary protein CD19 (Zipfel et al., 2000).

A model summarizing the different modes of c-Abl activation is shown in Figure 7. Starting from the regulated conformation of the kinase, c-Abl could be activated by either SH3 or SH2 domain ligands, leading to displacement of the inhibitory clamp from the backside of the kinase domain. Myristoyl displacement by a yet unidentified class of fatty-acid binding proteins might lead to a concomitant disruption of the SH2-kinase domain interface. These mechanisms might lead to a fully activated form of the kinase, which can be further stabilized, as well as initiated, by phosphorylation of the activation loop tyrosine Tyr-412 and/or Tyr-245 in the SH2-kinase linker (Plattner et al., 1999; Dorey et al., 2001; Brasher and Van Etten, 2000). Once phosphorylated, c-Abl can reassume its regulated state upon the action of cellular phosphatases (Cong et al., 2000).

We have previously found that the cap region could partly restore inhibition of a dimerization-defective form of the Bcr-Abl fusion protein (Pluk et al., 2002). This implies that regulatory constraints and activation modes as described in the model of Figure 7 may be operational within Bcr-Abl (Pluk et al., 2002; Sawyers, 2002). This view has now been prominently confirmed by an elegant genetic analysis revealing that mutations in all surfaces proposed to be participating in c-Abl regulation, including the cap, confer STI-571 resistance to Bcr-Abl (Azam et al., 2003 [this issue of *Cell*]). Residual regulatory constraints must therefore be operational within Bcr-Abl despite the lack of a myristoyl group and in competition to the activation caused by BCR-driven dimerization.

The crystal structure of the myristoylated form of c-Abl shows regions of electron density in the vicinity of the SH3 domain N terminus likely to represent interaction sites of the C-terminal part of the cap (functionally identified Lys-70 and Leu-73, Figure 4A; Nagar et al., 2003). The previously documented interaction of a GST-Cap fusion protein with the SH3-SH2 domain must mainly occur in this region. Phosphotyrosine-ligand activated c-Abl, in which the conformational restraints conferred by the SH3/SH2 clamp are not operational, is particularly sensitive to inhibition by STI-571. This suggests that "breathing" of the N-terminal and C-terminal lobes is an important parameter for the selectivity of protein kinase inhibitors, which may need to be "swallowed." These observations offer a potential explanation for the relative safety of STI-571 in treatment of leukemia patients. Since the developmental effects of loss of function of the *ABL1* or/and *ABL2* genes in the mouse are quite severe (Schwartzberg et al., 1991; Tybulewicz et al., 1991; Koleske et al., 1998), one could have anticipated toxicity problems through inhibition of the cellular form of the enzyme.

The myristoyl pocket appears to be quite specific for c-Abl and Arg as the corresponding space in Src kinases is filled with bulky side chains. It is possible that the

myristoyl binding pocket offers new opportunities for Bcr-Abl inhibitors since molecules that bind to it might be able to stabilize the inactive and assembled conformation of the enzyme.

Experimental Procedures

DNA Constructs

pSGT vector and pSGT-Abl constructs were previously described (Barilá and Superti-Furga, 1998). All point mutations and deletions were obtained using the quick-change site-directed mutagenesis kit (Stratagene) and pSGT-Abl 1b as template. All mutations were confirmed by sequencing.

Transfection and Immunoprecipitation

Transfection of HEK 293 cells and immunoprecipitation of Abl protein was carried out as described previously (Pluk et al., 2002). The relative concentration of immunoprecipitated Abl protein was determined by quantitative immunoblotting using the Odyssey system (Li-Cor) and normalized for c-Abl wild-type.

Abl Kinase Assay

Abl kinase assays were performed as described previously (Pluk et al., 2002). A peptide with the preferred c-Abl substrate sequence (Zhou et al., 1995) carrying an N-terminal biotin (biotin-GGEAIY AAPFKK-amide) was used as substrate. The terminated reaction was spotted onto a SAM2 Biotin Capture membrane (Promega) and further treated according to the manufacturer's instructions.

Isothermal Titration Calorimetry

Isothermal titration calorimetry (ITC) was performed using a VP-ITC machine (MicroCal). Abl kinase domain was purified as described previously (Nagar et al., 2002). Abl kinase domain:STI-571 complex and peptide samples (Myr-GQQPGKVLGDQRRPSL or NH2-GQQ PGKVLGDQRRPSL) were transferred to a buffer containing 20 mM Tris/HCl (pH 8.0), 150 mM NaCl, and 2 mM DTT. Titrations were performed at 25°C by injecting 20–25 consecutive aliquots of 10 μl of peptide solution (500 μM) into the ITC cell containing Abl:STI-571 complex (35–70 μM). The thermodynamic parameters of the reaction were determined by fitting the corrected data to a bimolecular interaction model.

Immunofluorescent Labeling and Microscopy

For immunofluorescence, VERO cells were fixed and permeabilized. Immunostaining was performed using anti-Abl antibodies (Ab-3, Oncogene Science, or K12, Santa Cruz). Secondary antibodies were coupled to Alexa-488 (Molecular Probes). Nuclei were counterstained with DAPI (Molecular Probes). F-actin was detected using rhodamine-conjugated phalloidin (Molecular Probes). Cells were imaged using a confocal microscope LSM510 (Zeiss).

Subcellular Fractionation

Transiently transfected HEK293 cells were resuspended in ice-cold swelling buffer (10 mM Tris-HCl [pH 7.5], 10 mM KCl, 1.5 mM MgCl2, 0.1 mM EDTA, and protease inhibitors). The actin cytoskeleton was depolymerized using 10 μM latrunculin A (Calbiochem). The remaining suspension was adjusted to 0.25 M sucrose and 1 mM EDTA. The nuclear fraction was obtained by centrifugation for 10 min at 10,600 × g. The postnuclear supernatant was centrifuged at 100,000 × g for 1 hr. The membrane pellet was solubilized in membane solubilization buffer (10 mM Tris-HCl (pH 7.9), 1 mM EDTA, 0.5% Triton X-100, and protease inhibitors), and insoluble material was removed by centrifugation.

Phosphopeptide Activation Assay

c-Abl wild-typet or Abl R171L was immunoprecipitated from total cell lysates using anti-Abl antibody. Phosphopeptide or control peptide was added to the immunoprecipitates at the indicated concentrations. The kinase assay was carried out as described previously (Pluk et al., 2002). Each experiment was normalized for a reaction performed in absence of peptide, and relative Abl activity was calculated.

Drug Inhibition Assay

c-Abl wild-type or Abl PP protein was immunoprecipitated from total cell extracts as described above. The immunoprecipitates were resuspended in kinase assay buffer (for the c-Abl wild-type and Abl PP control reactions) or kinase assay buffer containing 1 mM phosphopeptide in order to activate c-Abl. STI-571 was added at the indicated concentrations. The kinase assay was carried out as described previously (Pluk et al., 2002). Each experiment was normalized for a reaction in the absence of STI-571, and relative Abl activity was calculated.

Acknowledgments

We would like to thank J.R. Engen for early insights into the SH2-kinase domain interface; R. Pipkorn for expert synthesis of peptides; P. Riedinger for the c-Abl regulation cartoon; R. Pepperkok and the Advanced Light Microscopy Facility team at EMBL for support with confocal microscopy; R. Mangano, K. Scheffzek, and T. Stuwe for help and discussions; and A. Nebreda and R. Klein for critical reading of the manuscript. O.H. is supported by fellowships from the EMBL, the EMBO, and the Aventis Foundation. B.N. is supported by a fellowship of the Human Frontier Science Program. O.H. and S.G. are fellows of the German National Merit Foundation. Work in the G.S.F. laboratory is supported by the Cellzome AG and the EMBL.

Received: January 16, 2003
Revised: February 19, 2003

References

Azam, M., Latek, R.R., and Daley, G.Q. (2003). Mechanisms of autoinhibition and STI-157/imatinib resistance revealed by mutagenesis of *BCR-ABL*. Cell *112*, this issue, 831–843.

Barilá, D., and Superti-Furga, G. (1998). An intramolecular SH3-domain interaction regulates c-Abl activity. Nat. Genet. *18*, 280–282.

Barilá, D., Mangano, R., Gonfloni, S., Kretzschmar, J., Moro, M., Bohmann, D., and Superti-Furga, G. (2000). A nuclear tyrosine phosphorylation circuit: c-Jun as an activator and substrate of c-Abl and JNK. EMBO J. *19*, 273–281.

Blume-Jensen, P., and Hunter, T. (2001). Oncogenic kinase signaling. Nature *411*, 355–365.

Brasher, B.B., and Van Etten, R.A. (2000). c-Abl has high intrinsic tyrosine kinase activity that is stimulated by mutation of the src homology 3 domain and by autophosphorylation at two distinct regulatory tyrosines. J. Biol. Chem. *275*, 35631–35637.

Brasher, B.B., Roumiantsev, S., and Van Etten, R.A. (2001). Mutational analysis of the regulatory function of the c-Abl Src homology 3 domain. Oncogene *20*, 7744–7752.

Cong, F., Spencer, S., Cote, J.F., Wu, Y., Tremblay, M.L., Lasky, L.A., and Goff, S.P. (2000). Cytoskeletal protein PSTPIP1 directs the PEST-type protein tyrosine phosphatase to the c-Abl kinase to mediate Abl dephosphorylation. Mol. Cell *6*, 1413–1423.

Cox, S., Radzio-Andzelm, E., and Taylor, S.S. (1994). Domain movements in protein kinases. Curr. Opin. Struct. Biol. *4*, 893–901.

Daley, G.Q., Van Etten, R.A., Jackson, P.K., Bernards, A., and Baltimore, D. (1992). Nonmyristoylated Abl proteins transform a factor-dependent hematopoietic cell line. Mol. Cell. Biol. *12*, 1864–1871.

Dorey, K., Engen, J.R., Kretzschmar, J., Wilm, M., Neubauer, G., Schindler, T., and Superti-Furga, G. (2001). Phosphorylation and structure-based functional studies reveal a positive and a negative role for the activation loop of the c-Abl tyrosine kinase. Oncogene *20*, 8075–8084.

Druker, B.J., Tamura, S., Buchdunger, E., Ohno, S., Segal, G.M., Fanning, S., Zimmermann, J., and Lydon, N.B. (1996). Effects of a selective inhibitor of the Abl tyrosine kinase on the growth of Bcr-Abl positive cells. Nat. Med. *2*, 561–566.

Feller, S.M., Ren, R., Hanafusa, H., and Baltimore, D. (1994). SH2 and SH3 domains as molecular adhesives: the interactions of Crk and Abl. Trends Biochem. Sci. *19*, 453–458.

Furstoss, O., Dorey, K., Simon, V., Barila, D., Superti-Furga, G., and

Roche, S. (2002). c-Abl is an effector of Src for growth factor-induced c-myc expression and DNA synthesis. EMBO J. *21*, 514–524.

Gonfloni, S., Williams, J.C., Hattula, K., Weijland, A., Wierenga, R.K., and Superti-Furga, G. (1997). The role of the linker between the SH2 domain and catalytic domain in the regulation and function of Src. EMBO J. *16*, 7261–7271.

Gonfloni, S., Frischknecht, F., Way, M., and Superti-Furga, G. (1999). Leucine 255 of Src couples intramolecular interactions to inhibition of catalysis. Nat. Struct. Biol. *6*, 760–764.

Gonfloni, S., Weijland, A., Kretzschmar, J., and Superti-Furga, G. (2000). Crosstalk between the catalytic and regulatory domains allows bidirectional regulation of Src. Nat. Struct. Biol. *7*, 281–286.

Hardin, J.D., Boast, S., Mendelsohn, M., de los Santos, K., and Goff, S.P. (1996). Transgenes encoding both type I and type IV c-abl proteins rescue the lethality of c-abl mutant mice. Oncogene *12*, 2669–2677.

Hubbard, S.R. (1999). Structural analysis of receptor tyrosine kinases. Prog. Biophys. Mol. Biol. *71*, 343–358.

Hubbard, S.R. (2002). Protein tyrosine kinases: autoregulation and small-molecule inhibition. Curr. Opin. Struct. Biol. *12*, 735–741.

Hubbard, S.R., and Till, J.H. (2000). Protein tyrosine kinase structure and function. Annu. Rev. Biochem. *69*, 373–398.

Huse, M., and Kuriyan, J. (2002). The conformational plasticity of protein kinases. Cell *109*, 275–282.

Jackson, P., and Baltimore, D. (1989). N-terminal mutations activate the leukemogenic potential of the myristoylated form of c-abl. EMBO J. *8*, 449–456.

Koleske, A.J., Gifford, A.M., Scott, M.L., Nee, M., Bronson, R.T., Miczek, K.A., and Baltimore, D. (1998). Essential roles for the Abl and Arg tyrosine kinases in neurulation. Neuron *21*, 1259–1272.

Liu, X., Brodeur, S.R., Gish, G., Songyang, Z., Cantley, L.C., Laudano, A.P., and Pawson, T. (1993). Regulation of c-Src tyrosine kinase activity by the Src SH2 domain. Oncogene *8*, 1119–1126.

Manning, G., Whyte, D.B., Martinez, R., Hunter, T., and Sudarsanam, S. (2002). The protein kinase complement of the human genome. Science *298*, 1912–1934.

Mayer, B.J., Jackson, P.K., Van Etten, R.A., and Baltimore, D. (1992). Point mutations in the abl SH2 domain coordinately impair phosphotyrosine binding in vitro and transforming activity in vivo. Mol. Cell. Biol. *12*, 609–618.

McWhirter, J.R., Galasso, D.L., and Wang, J.Y. (1993). A coiled-coil oligomerization domain of Bcr is essential for the transforming function of Bcr-Abl oncoproteins. Mol. Cell. Biol. *13*, 7587–7595.

Moarefi, I., LaFevre-Bernt, M., Sicheri, F., Huse, M., Lee, C.H., Kuriyan, J., and Miller, W.T. (1997). Activation of the Src-family tyrosine kinase Hck by SH3 domain displacement. Nature *385*, 650–653.

Musacchio, A., Saraste, M., and Wilmanns, M. (1994). High-resolution crystal structures of tyrosine kinase SH3 domains complexed with proline-rich peptides. Nat. Struct. Biol. *1*, 546–551.

Nagar, B., Bornmann, W.G., Pellicena, P., Schindler, T., Veach, D.R., Miller, W.T., Clarkson, B., and Kuriyan, J. (2002). Crystal structures of the kinase domain of c-Abl in complex with the small molecule inhibitors PD173955 and imatinib (STI-571). Cancer Res. *62*, 4236–4243.

Nagar, B., Hantschel, O., Young, M.A., Scheffzek, K., Veach, D., Bornmann, W., Clarkson, B., Superti-Furga, G., and Kuriyan, J. (2003). Structural basis for the autoinhibition of c-Abl tyrosine kinase. Cell *112*, this issue, 859–871.

Pendergast, A.M. (2002). The Abl family kinases: mechanisms of regulation and signaling. Adv. Cancer Res. *85*, 51–100.

Plattner, R., Kadlec, L., DeMali, K.A., Kazlauskas, A., and Pendergast, A.M. (1999). c-Abl is activated by growth factors and src family kinases and has a role in the cellular response to PDGF. Genes Dev. *13*, 2400–2411.

Pluk, H., Dorey, K., and Superti-Furga, G. (2002). Autoinhibition of c-Abl. Cell *108*, 247–259.

Porter, M., Schindler, T., Kuriyan, J., and Miller, W.T. (2000). Reciprocal regulation of Hck activity by phosphorylation of Tyr(527) and Tyr(416). Effect of introducing a high affinity intramolecular SH2 ligand. J. Biol. Chem. *275*, 2721–2726.

Raitano, A.B., Whang, Y.E., and Sawyers, C.L. (1997). Signal transduction by wild-type and leukemogenic Abl proteins. Biochim. Biophys. Acta *1333*, F201–F216.

Renshaw, M.W., Capozza, M.A., and Wang, J.Y. (1988). Differential expression of type-specific c-abl mRNAs in mouse tissues and cell lines. Mol. Cell. Biol. *8*, 4547–4551.

Resh, M.D. (1994). Myristylation and palmitylation of Src family members: the fats of the matter. Cell *76*, 411–413.

Resh, M.D. (1999). Fatty acylation of proteins: new insights into membrane targeting of myristoylated and palmitoylated proteins. Biochim. Biophys. Acta *1451*, 1–16.

Roumiantsev, S., Shah, N.P., Gorre, M.E., Nicoll, J., Brasher, B.B., Sawyers, C.L., and Van Etten, R.A. (2002). Clinical resistance to the kinase inhibitor STI-571 in chronic myeloid leukemia by mutation of Tyr-253 in the Abl kinase domain P-loop. Proc. Natl. Acad. Sci. USA *99*, 10700–10705.

Roussel, R.R., Brodeur, S.R., Shalloway, D., and Laudano, A.P. (1991). Selective binding of activated pp60c-src by an immobilized synthetic phosphopeptide modeled on the carboxyl terminus of pp60c-src. Proc. Natl. Acad. Sci. USA *88*, 10696–10700.

Sawyers, C.L. (2002). Disabling Abl-perspectives on Abl kinase regulation and cancer therapeutics. Cancer Cell *1*, 13–15.

Schindler, T., Bornmann, W., Pellicena, P., Miller, W.T., Clarkson, B., and Kuriyan, J. (2000). Structural mechanism for STI-571 inhibition of abelson tyrosine kinase. Science *289*, 1938–1942.

Schlessinger, J. (2000). Cell signaling by receptor tyrosine kinases. Cell *103*, 211–225.

Schwartzberg, P.L., Stall, A.M., Hardin, J.D., Bowdish, K.S., Humaran, T., Boast, S., Harbison, M.L., Robertson, E.J., and Goff, S.P. (1991). Mice homozygous for the ablm1 mutation show poor viability and depletion of selected B and T cell populations. Cell *65*, 1165–1175.

Sicheri, F., Moarefi, I., and Kuriyan, J. (1997). Crystal structure of the Src family tyrosine kinase Hck. Nature *385*, 602–609.

Smith, J.M., and Mayer, B.J. (2002). Abl: mechanisms of regulation and activation. Front. Biosci. *7*, d31–42.

Superti-Furga, G., and Courtneidge, S.A. (1995). Structure-function relationships in Src family and related protein tyrosine kinases. Bioessays *17*, 321–330.

Taagepera, S., McDonald, D., Loeb, J.E., Whitaker, L.L., McElroy, A.K., Wang, J.Y., and Hope, T.J. (1998). Nuclear-cytoplasmic shuttling of C-ABL tyrosine kinase. Proc. Natl. Acad. Sci. USA *95*, 7457–7462.

Taniguchi, H. (1999). Protein myristoylation in protein-lipid and protein-protein interactions. Biophys. Chem. *82*, 129–137.

Taylor, S.S., and Radzio-Andzelm, E. (1997). Protein kinase inhibition: natural and synthetic variations on a theme. Curr. Opin. Chem. Biol. *1*, 219–226.

Tybulewicz, V.L.J., Crawford, C.E., Jackson, P.K., Bronson, R.T., and Mulligan, R.C. (1991). Neonatal lethality and lymphopenia in mice with a homozygous disruption of the c-*abl* proto-oncogene. Cell *65*, 1153–1163.

Van Etten, R.A. (1999). Cycling, stressed-out and nervous: cellular functions of c-Abl. Trends Cell Biol. *9*, 179–186.

Van Etten, R.A., Jackson, P.K., Baltimore, D., Sanders, M.C., Matsudaira, P.T., and Janmey, P.A. (1994). The COOH terminus of the c-Abl tyrosine kinase contains distinct F- and G-actin binding domains with bundling activity. J. Cell Biol. *124*, 325–340.

Williams, J.C., Weijland, A., Gonfloni, S., Thompson, A., Courtneidge, S.A., Superti-Furga, G., and Wierenga, R.K. (1997). The 2.35 Å crystal structure of the inactivated form of chicken Src: a dynamic molecule with multiple regulatory interactions. J. Mol. Biol. *274*, 757–775.

Woodring, P.J., Litwack, E.D., O'Leary, D.D., Lucero, G.R., Wang, J.Y., and Hunter, T. (2002). Modulation of the F-actin cytoskeleton by c-Abl tyrosine kinase in cell spreading and neurite extension. J. Cell Biol. *156*, 879–892.

Xu, W., Harrison, S.C., and Eck, M.J. (1997). Three-dimensional structure of the tyrosine kinase c-Src. Nature *385*, 595–601.

Yano, H., Cong, F., Birge, R.B., Goff, S.P., and Chao, M.V. (2000). Association of the Abl tyrosine kinase with the Trk nerve growth factor receptor. J. Neurosci. Res. *59*, 356–364.

Young, M.A., Gonfloni, S., Superti-Furga, G., Roux, B., and Kuriyan, J. (2001). Dynamic coupling between the SH2 and SH3 domains of c-Src and Hck underlies their inactivation by C-terminal tyrosine phosphorylation. Cell *105*, 115–126.

Yu, H.H., Zisch, A.H., Dodelet, V.C., and Pasquale, E.B. (2001). Multiple signaling interactions of Abl and Arg kinases with the EphB2 receptor. Oncogene *20*, 3995–4006.

Zhou, S., Carraway, K.L., 3rd, Eck, M.J., Harrison, S.C., Feldman, R.A., Mohammadi, M., Schlessinger, J., Hubbard, S.R., Smith, D.P., Eng, C., et al. (1995). Catalytic specificity of protein-tyrosine kinases is critical for selective signalling. Nature *373*, 536–539.

Zhu, G., Decker, S.J., Maclean, D., McNamara, D.J., Singh, J., Sawyer, T.K., and Saltiel, A.R. (1994). Sequence specificity in the recognition of the epidermal growth factor receptor by the abl Src homology 2 domain. Oncogene *9*, 1379–1385.

Zipfel, P.A., Grove, M., Blackburn, K., Fujimoto, M., Tedder, T.F., and Pendergast, A.M. (2000). The c-Abl tyrosine kinase is regulated downstream of the B cell antigen receptor and interacts with CD19. J. Immunol. *165*, 6872–6879.